Proceedings of the Seventh IASTED International Conference
POWER AND ENERGY SYSTEMS
August 29–31, 2007, Palma de Mallorca, Spain
ISBN Hardcopy: 978-0-88986-689-8 / CD: 978-0-88986-690-4

PERFORMANCE EVALUATION OF PERMANENT MAGNET SYNCHRONOUS MOTOR/GENERATOR FOR SUPERCONDUCTOR FLYWHEEL ENERGY STORAGE SYSTEMS

*Jeong-Phil Lee, *Tae-Hyun Sung, *Se-Yong Jung, *Young-Hee Han, **Dae-Jun You, **Seok-Myeong Jang
* Korea Electric Power Energy Research Institute, ** Chung -Nam National University
* 103-16 Munji-Dong, Yuseong-Gu, Daejeon 305-380
** 220 Gung-Dong Yuseong-Gu, Daejoen, 305-764
Korea
jplee@kepri.re.kr

ABSTRACT
The rotational loss is one of the most important problems for the practical use of superconductor flywheel energy storage system. The rotational loss of the SFES is mainly generated in the part of magnetic field such as superconductor bearing and motor/generator. The rotational loss of PM type motor/generator is much larger than that of superconductor bearing. So the motor must be designed in accordance with application object of flywheel energy storage system as well as the required power. In this paper, permanent magnet synchronous motor (PMSM) for superconductor flywheel energy storage systems is designed by analytical method of magnetic field and dynamic modeling. This design model consists of the surface-mounted PM rotor with diametrical magnetization and slotless iron-cored stator. And, its performance is evaluated in motoring and idling mode considering the required power and core loss. The results show that the design of PMSM to satisfy the required power and the calculation of core loss can be accomplished by the analytical solution through magnetic field analysis.

KEY WORDS
Superconductor Flywheel Energy Storage System (SFES), Rotational loss, Superconductor bearing, Motor/generator, idling loss, permanent magnet synchronous motor (PMSM)

1. Introduction

The SFES(Superconductor Flywheel Energy Storage System) is energy storage equipment which can be used by electrical energy when needed, after electrical energy is stored into mechanical rotational energy. The mean difference of electrical energy demand of day and night reaches about 30%. This difference is larger in summer because of use of an air conditioner in Korea. But it is difficult to increase the generating equipment and is inefficient to increase the generating plant for these conditions. The SFES is can be used by spinning reserve at peak loading through surplus electric power storing of midnight to cope with inefficient energy consumption system and is environment-friendly energy storage system which can be used by uninterrupted power supply and storage of distributed resources such as solar power and wind power.

The SFES using high temperature superconductor bearing hardly have a friction loss unlike mechanical bearing. Thus the efficiency and the density of energy storage is much high. Generally rotational loss is necessarily generated due to friction between rotor and stator in mechanical bearing and the loss is much high. But because of no contact between rotor and stator through the use of superconductor bearing using magnetic levitation and magnetic pinning force which is special phenomenon of high temperature superconductor, the rotational loss can be decreased very much. Nevertheless, many factors which decrease rotational speed are included in the SFES.

Because electrical energy is converted into rotational energy of flywheel, if rotational speed of flywheel decrease, stored energy also decrease. Thus energy storage efficiency lowers. So much rotational speed reduction can be critical weak point of the SFES which stores energy for a long time.

In order to minimize rotation loss which can be generated in the middle of rotation, it is needed to assess loss mechanism which is generated in various parts of the SFES. The rotational loss of the SFES is generated in the part of magnetic field such as superconductor bearing and motor/generator. The rotational loss of superconductor bearing is generated by the induced current in the superconductors by inhomogeneous field of the permanent magnetic rotor and the eddy current in the PM rotor induced by the magnetic filed of the superconductor[1][2]. And the rotational loss of motor/generator of the SFES is generated by eddy current loss and hysterisis loss in the core of motor/generator due to rotation of magnetic field of the permanent magnetic rotor. Generally the rotational loss of PM type motor/generator is much larger than that of superconductor bearing[3]. To improve storage efficiency of the SFES, the loss of PM type motor/generator for the

SFES must be minimized. The motor must be designed in accordance with application object of flywheel energy storage system. To do this, the loss characteristics of PM type motor/generator must be assessed.

In this paper, the performance of permanent magnet synchronous motor (PMSM) for superconductor flywheel energy storage systems is evaluated. The operation modes of the SFES have 3 modes such as motoring, idling and generating. So the losses of the SFES are also generated motoring loss, idling loss and generating loss.
In motoring mode, PMSM is designed to satisfy 10[kW] – 20,000[rpm]. In the PMSM design, it is determined by volume of permanent magnet and turns of winding by electromagnetic analysis. Slotless type is selected to reduce iron loss (hysterisis and eddy current loss) and loss by vibration. In idling mode, design method to reduce iron loss and analytical method to predict iron loss are proposed.

2. kWh-class Superconductor Flywheel Energy Storage System

2.1 SFES system

The schematic view of manufactured 5 kWh class SFES is shown in Fig. 1, where stator of superconductor bearing is located at the upper part and the lower part of flywheel. Stator of superconductor bearing is composed of YBCO bulk superconductor. Permanent magnetic of flywheel rotor is surrounded with this journal type bearing. The whole flywheel rotor weights 215kg. To lift this flywheel by only superconductor bearing, number of the superconductor YBCO bulk must increase. This increases the superconductor bearing size and the cost for cooling and vacuum. So it is designed to support partial flywheel weight using FMB(Floating Magnetic Bearing) and stable levitation of flywheel using superconductor bearing, where superconductor bearing is cooled by LN2 circulation

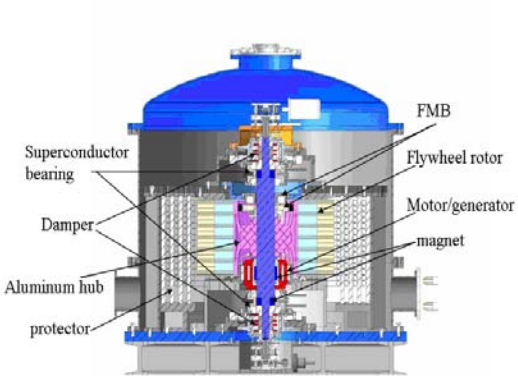

Fig. 1 Schematic view of 5 kWh-class SFES

The active magnetic dampers are installed at the upper part and the lower part of the SFES to stabilize the high speed rotation. These all parts are installed in vacuum chamber to minimize rotational loss and cooling loss.

2.2 Superconductor bearing

Superconductor bearing for 5 kWh-class SFES is shown in Fig. 2. 8 YBCO bulk superconductors are installed in one stator of superconductor bearing. YBCO bulk is cooled by LN2. The bearing is designed that the distance between superconductor and permanent magnet become 5mm. In order to reduce eddy current loss, metal is not used in 100G magnetic field. Inner side of cryostat is made of G-10 to reduce eddy current loss.

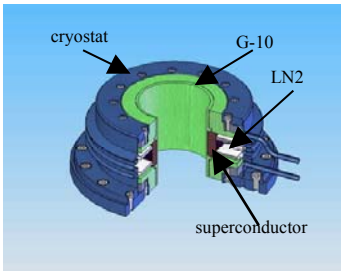

Fig. 2 Superconductor Bearing for 5 kWh-class SFESS

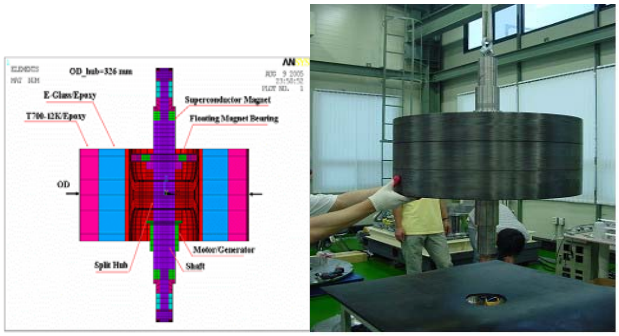

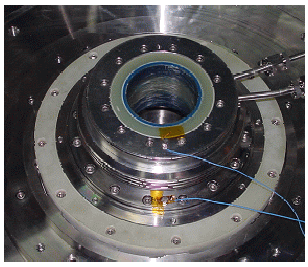
Fig 3. Flywheel rotor for 5 kWh-class SFES

2.3 Flywheel rotor

The construction of rotor is shown in Fig. 3. The flywheel rotor is composed of titanium shaft, aluminium hub, composite wheel, magnet ring set for superconductor bearing, floating magnet and permanent magnet for motor/generator, etc.

3. Design of Motor/generator

3.1 Field analysis by permanent magnet rotor

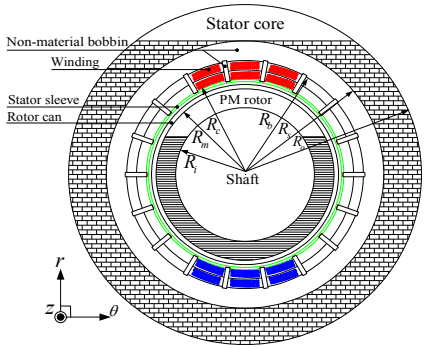

Fig. 4 PMSM motor/generator with 2-pole and 3-phase winding (10KW)

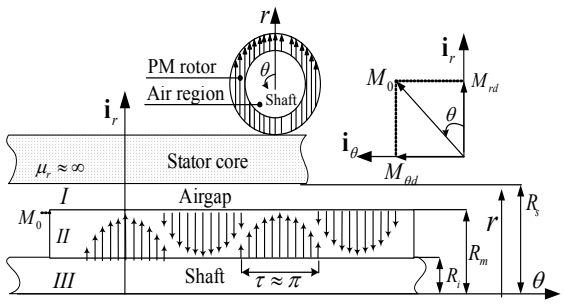

Fig. 5 Modeling and analytical frame of diametrically magnetized PM rotor

In order to facilitate the design optimization and dynamic modeling of PM synchronous machines as shown in Fig. 4, a variety of techniques such as the lumped equivalent circuit and the numerical method have been employed to predict the magnetic field distribution for design parameters. However, they do not provide as much insight as analytical solutions into the influence of the design parameters on the optimum design procedures. Therefore, this paper offers a two-dimensional analytical solution which can treat distribution of magnetized materials to satisfy the power and evaluate the core loss.

The geometry used to model the motor fields is idealized as a two-dimensional structure as shown in Fig. 5. Here, the lower region of thickness (R_m-R_i) represents the PM rotor with the diametrical magnetization. The upper region is the slotless stator with laminated iron core. Thus R_s-R_m is height of the motor air gap. Such a promising motor structure, PM rotor can be predicted that diametrical magnetization has both radial and θ-components. As a consequence, the Fourier series expansion of diametrical magnetization can be expressed as [4]

$$\mathbf{M} = M_{rd}\mathbf{i}_r + M_{\theta d}\mathbf{i}_\theta \tag{1}$$

Where

$$M_r \approx M_0 \cos\theta \text{ and } M_\theta \approx -M_0 \sin\theta \tag{2}$$

here, θ represents angular position referred to rotor and the magnetization amplitude M_o of PM is given by B_r/μ_o from the remanence B_r of NdFeB35 material and permeability μ_o with air region. Moving direction of the machines is assumed to be infinite in θ -direction. For the theoretical aspects of this paper, Maxell's equations for magnetic vector potential **A** and flux density **B** inside PM and air region are [5]

$$\begin{cases} \mathbf{B} = \nabla \times \mathbf{A} \\ \nabla \times \mathbf{B} = 0 \text{ (inside air region)} \\ \nabla \times \mathbf{B} = \mu_0 (\nabla \times \mathbf{M}) \text{ (inside PM region)} \\ \nabla \cdot \mathbf{B} = \mathbf{0} \end{cases} \tag{3}$$

where $\mu_0 = 4\pi \times 10^{-7}$ H/m is the permeability of free space. We assume the permeability to be μ_0 inside PM and air region since its relative permeability is near unity. And the magnetic vector potential is defined by $A_{zd} = A(r)\, e^{-jq\theta}$ with $q = \pi/\tau$ and θ -directed rotation. Thus, the magnetic vector potential is purely z-directed in current direction. Therefore, from terms of Coulomb gauge $\nabla \cdot \mathbf{A} = 0$, the vector Poisson equation of PM and air regions simplifies to the scalar relationship as follow

$$\begin{cases} \dfrac{d^2 A_{zd}^I}{dr^2} + \dfrac{1}{r}\dfrac{dA_{zd}^I}{dr} - \dfrac{q^2}{r^2} A_{zd}^I = 0 \text{ (inside air region)} \\ \dfrac{d^2 A_{zd}^{II}}{dr^2} + \dfrac{1}{r}\dfrac{dA_{zd}^{II}}{dr} - \dfrac{q^2}{r^2} A_{zd}^{II} = -j\mu_0 \dfrac{q}{r} M_{rd} \text{ (inside PM region)} \end{cases} \tag{4}$$

In order to solve the field quantities by PM magnetization, the boundary conditions on field and potential at each of the four boundaries are applied. Since equivalent current for θ –components of diametrical magnetization is discontinuous at the PM surface, θ-components of magnetization is considered by applying Ampere's law. And, due to assuming that the permeability of stator core is infinite, the θ-components of field intensity is zero at $r = R_s$. Also, the magnetic vector potential does not exist at center of the rotating machines. As a consequence, boundary conditions in design model of Fig.4 are given by[4]

$$\begin{cases} A_{zd}^{III}(r,\theta)\big|_{R_i=0} = 0 \\ B_{\theta d}^{II}(r,\theta)\big|_{r=R_i} - B_{\theta d}^{III}(r,\theta)\big|_{r=R_i} = \mu_0 M_{\theta d} \\ B_{\theta d}^{II}(r,\theta)\big|_{r=R_m} - B_{\theta d}^{I}(r,\theta)\big|_{r=R_m} = \mu_0 M_{\theta d} \\ B_{\theta d}^{I}(r,\theta)\big|_{r=R_s} = 0 \end{cases} \tag{5}$$

From (4) and (5), the radial and θ-component of flux density due to permanent magnets in the air-gap region I is obtained as follow

$$\begin{cases} B_{rd}^I = \dfrac{B_r}{2(R_s r)^2}(R_s^2 + r^2)(R_m^2 - R_i^2)\cos\theta \\ B_{\theta d}^I = \dfrac{B_r}{2(R_s r)^2}(R_s^2 - r^2)(R_m^2 - R_i^2)\sin\theta \end{cases} \tag{6}$$

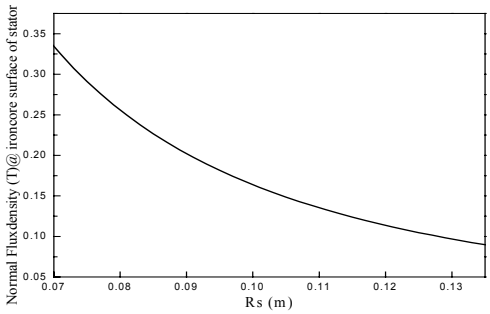

Fig. 6 Normal flux density (T) at surface of stator core according to variation of R_s

As the results of (6), Fig. 6 shows the normal flux density at surface of stator core according to variation of inner radius Rs in stator core. Here, we selected the design point at surface flux density 0.2(T) for reducing eddy current by magnetic field of PM rotor.

3.2 Dynamic analysis of PMLSM for operating range

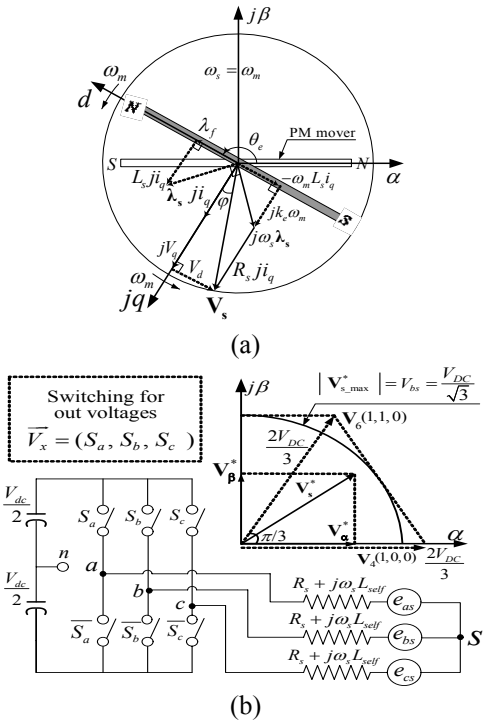

Fig. 7 Dynamic analysis in steady state: (a) phasor diagram in motoring, (b) Relation between reference and DC link voltage considering switching scheme of inverter.

In the design model of Fig. 4, the electrical dynamic equation of a typical surface-mounted PMLSM can be described from modeling of 3-phase winding in rotating time domain as follow

$$\begin{bmatrix} V_{as}(\omega_s t) \\ V_{bs}(\omega_s t) \\ V_{cs}(\omega_s t) \end{bmatrix} = \begin{bmatrix} R + pL_{self} & pM & pM \\ pM & R + pL_{self} & pM \\ pM & pM & R + pL_{self} \end{bmatrix} \begin{bmatrix} i_{as}(\omega_s t) \\ i_{bs}(\omega_s t) \\ i_{cs}(\omega_s t) \end{bmatrix} + \begin{bmatrix} e_{as}(\omega_s t) \\ e_{bs}(\omega_s t) \\ e_{cs}(\omega_s t) \end{bmatrix} \quad (7)$$

where V_{as}, V_{bs}, V_{cs} are the input phase voltages, i_{as}, i_{bs}, i_{cs} are the phase currents, e_{as}, e_{bs}, e_{cs} are the phase Back-emf voltages by migration velocity of PM mover on moving stage which are driven by stator coils in the fixed machine base, and p represents d/dt. From this electric circuit modeling, we can define the resistance R and the self-inductance L_{self} including leakage inductance L_l of one phase as design parameters. In particular, since the mutual inductance M between two phases is displaced by 120 electrical degrees, it can be calculated by adding up the linkage flux of a second coil placed in the field of the first one.

The Back-emf voltage induced in 3-phase winding due to the magnet flux crossing the air gap is found by applying the linkage flux $\lambda_{(pm)}$ by normal flux density of PM rotor. Considering only the fundamental component, the linkage flux of 3- phase stator winding by PM mover flux are written as

$$\lambda_{(pm)} = \lambda_f \cos\theta_i, (\theta_i = \theta, \theta - \frac{2\tau}{3}, \theta - \frac{4\tau}{3}) \quad (8)$$

here λ_f is the peak value of the linkage flux in sinusoidal wave form. $\theta_e = \int \omega_s dt$ and $\theta_e = -\int \omega_s dt$ for rotor position from the fixed stator in initial position, which ω_s is an electric angle frequency of PM mover. The significance of this linkage flux is that it induces a voltage across the winding whenever the linkage flux varies with time. Hence, the Back- emf is given by Faraday's law and Lenz's law, which states

$$e_s(\omega_s t) = -\frac{d\lambda_{(pm)}}{dt} = \omega_s \lambda_f \sin\theta_i \quad (9)$$

This mathematical projection greatly simplifies the expression of the electrical dynamic equation and removes dependencies of their time and position. Hence, under steady state, the dq-model equation by Clark & Park's transformation are given by [6]

$$\begin{bmatrix} V_d \\ V_q \end{bmatrix} = \begin{bmatrix} R_s + pL_s & -\omega_m L_s \\ \omega_m L_s & R_s + pL_s \end{bmatrix} \begin{bmatrix} i_d \\ i_q \end{bmatrix} + \begin{bmatrix} 0 \\ \lambda_f \omega_m \end{bmatrix} \quad (10)$$

In the electrical power delivered to the motor by input voltage, a part of it is transformed in Joule losses, another part are defined as the reactive power by magnetic conversion of electric energy, and last part is used in mechanical energy. That is

$$P_{input} = \frac{3}{2}(V_d i_d + V_q i_q) = P_{loss} + P_{reactive} + P_{mech} \quad (11)$$

In particular, the electric thrust from the mechanical energy is calculated as follow [6]

$$F_e = \frac{P_{mech}}{\omega_m} = \frac{3}{2}(\lambda_f i_q) = 1.5\lambda_f i_q = k_t i_q \quad (12)$$

here 3/2 is the compensation coefficient for energy definition in dq-transformation process. In mechanical energy by current control, the electric thrust F_e only varies with i_q. It is shown that the direct q-current by dq-transformation enables a continuous control of thrust demand without ripple.

In the case of a static power bridge, the direct sinusoidal

voltage sources are not used for speed control according to load. They are replaced by 6 power transistors that act on/off switches to the rectified DC link voltages as shown in Fig. 7(b), which, switching (S_a, S_b, S_c) by digital controller recreate a sinusoidal current in the coils and generate the rotating field. Here, using the virtual middle point n of rectified voltage, the relation of switching and DC link voltage V_{DC} are calculated as

$$\begin{aligned} V_{an} &= (V_{DC}/2)(2S_a - 1_c) \\ V_{bn} &= (V_{DC}/2)(2S_b - 1_a) \\ V_{cn} &= (V_{DC}/2)(2S_c - 1_b) \end{aligned} \tag{13}$$

And, from the pole voltage (V_{an}, V_{bn}, V_{cn}) and the offset voltage V_{sn}, equation of the phase voltage and switching including DC link voltage are obtained by

$$\begin{aligned} V_{as} &= (V_{DC}/3)(2S_a - S_b - S_c) \\ V_{bs} &= (V_{DC}/3)(2S_b - S_c - S_a) \\ V_{cs} &= (V_{DC}/3)(2S_c - S_a - S_b) \end{aligned} \tag{14}$$

here V_{as}, V_{bs}, V_{cs} are the phase voltage with PWM, respectively. For one such the applied voltage with digital switching, we adopt the Space Vector PWM (SVPWM) providing more efficient use of the DC bus voltage and less harmonic distortion than direct sinusoidal modulation technique. The objective of SVPWM technique is approximately to supply electric energy from the time combination of adjacent switching patterns for the reference voltage vector $\mathbf{V}_s^*$ as shown in Fig. 7(b). Therefore, in effort to obtain rotating reference vector from adjacent switching, the maximum voltage vector $\mathbf{V}_{\mathrm{smax}}$ of one phase are restricted by DC link voltage as follow

$$\left|\mathbf{V}^*_{s\max}\right| = V_{bs} = \frac{1}{\sqrt{3}} V_{DC} \tag{15}$$

where $1/\sqrt{3}$ is the significant design parameter for applying the electrical energy from inverter with SVPWM technique. From the restriction of input voltage by determination of a DC link voltage, The base speed is defined as synchronous speed at which the back-emf reaches the maximum permissible value along the maximum thrust vs. speed envelop. Therefore, from electrical dynamic equation with base thrust F_{bs} by maximum current $i_{q\max}$ and Back-emf by base speed ω_{bs}, the base voltage V_{bs} for maximum operating are given by

$$V_{bs} = \left|V_{dbs} + jV_{qbs}\right| = \frac{V_{DC}}{\sqrt{3}} = \sqrt{\left(-\frac{\omega_{bs} L_s F_{bs}}{k_t}\right)^2 + \left(R_s \frac{F_{bs}}{k_t} + \lambda_f \omega_{bs}\right)^2} \tag{16}$$

3.3 Procedure of PMSM design and FEM verification

In order to design the PMSM system, we have first studied magnetic field analysis. And operating range of system is calculated by design parameters of PMLSM and a DC link voltage for providing input power from inverter. Thus, in this section, we offers the design procedure of PMSM to satisfy the required power considering design parameters within the scope of base value defined as maximum operating as shown in Fig. 8.

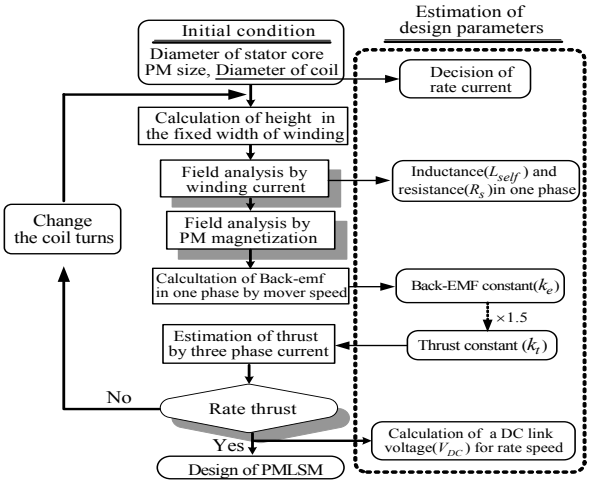

Fig.8 Design procedure of PMSM with slotless stator

Table. 1 Design geometry of the manufactured PMSM

Design geometry		Value
Shaft radius	R_i	46 (mm)
PM outer radius	R_m	59 (mm)
Stator inner radius	R_s	92 (mm)
One-phase turns	N	96 ($turns$)
Flux-linkage by PM	λ_f	0.158 (V/sec)
One-phase resistance	R	0.248(Ω)
Self Inductance	L_{self}	17.42(mH)

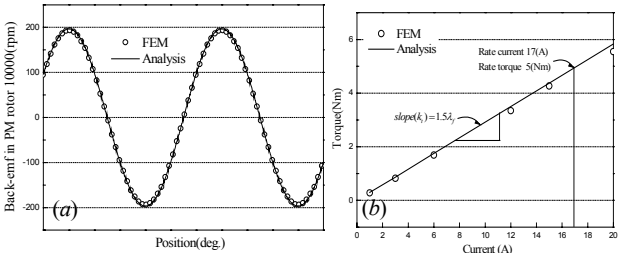

Fig. 9 FEM verification of (a) Back-emf of one-phase winding at PM rotor 10000(rpm) and (b) Torque vs. current

As a first design procedure to satisfy, we have selected the initial condition such as Diameter of stator core, PM size and coil diameter which is related to core loss and motor size. And then, the design parameters for the base thrust is obtained from the magnetic field analysis by PM magnetization and winding current according to variation of coil turns. Finally, the DC link voltage for base speed is calculated by dynamic analysis including design parameters and base thrust. In this paper, the DC link voltage is given in 300(V). Table.I shows the design geometry of the manufactured PMSM by the selection of winding turns 96(turns). And Fig. 9 presents the FEM

verification to satisfy the required power 10 (KW). Here, the Back-emf is restricted by the DC link voltage at PM rotor speed 20000(rpm). And the torque is obtained from wire diameters 1.8(*mm*) in electric restriction.

4. Evaluation of the loss in the idling mode

The loss in idling mode is generated in stator core by permanent magnet rotor. Amount of loss depend on the core material and its lamination thickness. The material of steel is selected by means of iron loss data and data sheet which is given by manufacture company. Iron loss data for Arnon 7 of Arnold Magnetic Technologies Corporation is shown in Fig. 10. Arnon series steel is high performance magnetic material which is very lower iron loss in high frequency. Thickness is 0.15mm, coating is from 0.00004 inch to 0.00015 inch, and its insulation performance is the minimum of 10 $\Omega - cm^2 / lam$

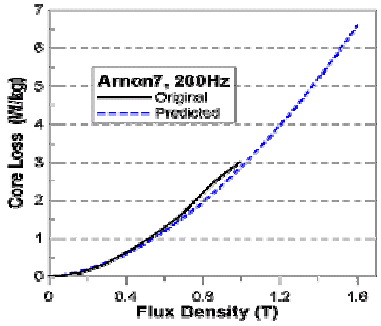

Fig. 10 Core loss data for Arnon 7

To estimate iron loss coefficient easily in modified Steinmetz equation using the data given in Fig. 7, the expression divided by frequency f is given by equation (17)

$$P_c / f = k_h B^n + k_e f B^2 + k_a \sqrt{f} B^{1.5} \quad (17)$$

where k_h , k_e and n are hysterisis coefficient, eddy current coefficient and Steinmetz constant respectively. k_a is anomalous eddy current coefficient, which is related to the material thickness, cross-sectional area and conductivity.

The coefficient of iron loss for each frequency using data given in Fig 10 is shown in Fig. 11. Each figure is given by equation (17) using real data. This represents continuous loss coefficient by curve fitting function. The core loss according to rotational speed of motor designed in idling mode is shown in Fig 12. The iron loss is about 18[W] in 20000[rpm] of the operation speed of the SFES.

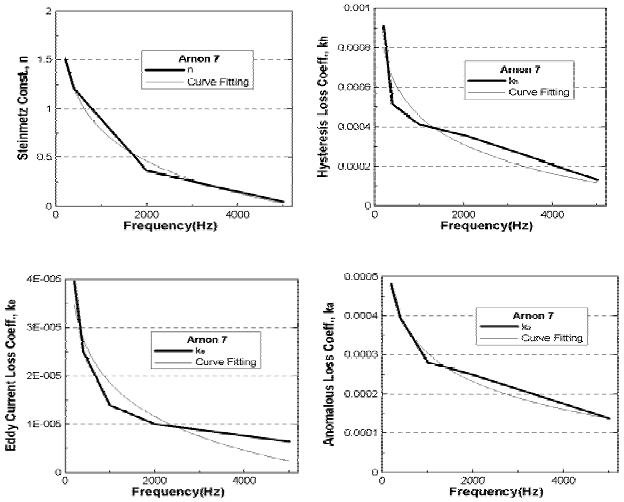

Fig. 11 Estimation of coefficient by iron loss data

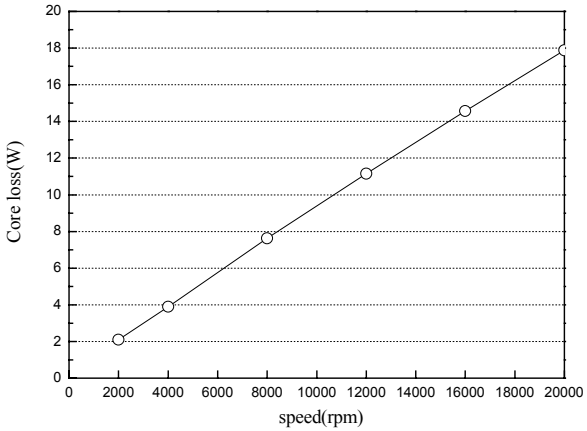

Fig. 12 Core loss according to speed

5. Conclusion

Generally, the design of the PMSM is performed to satisfy the required power composed of the Back-emf and torque. Although this focus is important, the core loss and vibration must be considered for application in SFES. Therefore, this paper dealt with the design of PMSM to satisfy the required power and calculation of core loss to evaluate the idling mode. In approach of PMSM design, the estimation of magnetic field is significant key to evaluate the required power and core loss. Moreover, the calculation of core loss can determine the application range whether SFES is used for UPS or for long lasting storage. The magnetic field analysis in this paper can contribute to PMSM design for SFES.

References

[1] K. Demachi, K. Miya, R. Takakata, H. Kameno and H. Higasa, Numerical evaluation of rotation speed degradation of superconducting magnetic bearing caused by the electromagnetic phenomena, *Phisica C*, 378-381, 2002, 858-863.

[2] I. Massie, K. Demachi, T. Ichihara and M. Uesaka, Rotational loss modelling in superconducting magnetic

bearing, *IEEE Tans. On Applied Superconductivity*, 16(2), 2006, 1807-1810
[3] A. C. Day, J. R. Hull, M. Strasik, P. E. Johnson, Kevin E. McCray, J. Edwards, J. A. Mittleider, J. R. Schindler, R. A. Hawkins, and N, K, Yoder, Temperature and frequency effects in a high-performance superconducting bearing, *IEEE Trans. On Applied Superconductivity*, 13(2), 2003, 2179-2184
[4] S.M. Jang, J.Y Choi, D.J. You and H.S. Young , Electromagnetic analysis of high speed machines with diametrically magnetized rotor, considering slotting effect and applied to new magnetization modeling, IEEE IEMDC conference, 2005
[5] J.R. Melcher, Continuum Electromechanics, *Cambridge, MA:MIT Press*, 1981.
[6] Erwan Simon, Implementation of a Speed Field Oriented Control of 3-phase PMSM Motor using TMS320F240 *Texas Instruments application report*, SPRA588, 1999